**Supplementary Information**

# Development of pathway-oriented screening to identify compounds to control 2-methylglyoxal metabolism in tumor cells

Kouichi Yanagi, Toru Komatsu, Yuuta Fujikawa, Hirotatsu Kojima, Takayoshi Okabe, Tetsuo Nagano, Tasuku Ueno, Kenjiro Hanaoka and Yasuteru Urano

## Contents



## Supplementary data for preparation of compounds

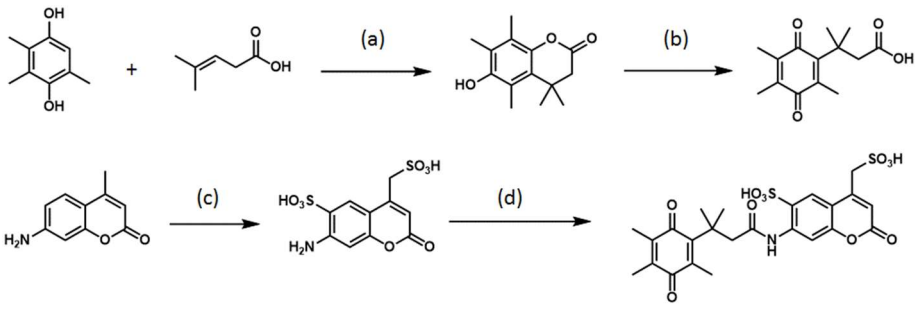


**Scheme S1.** Preparation of Q-dsAMC. (a) $MeSO_3H$, 85°C, Yield: quant. (b) NBS, $MeCN/H_2O$, r.t., Yield: 76.7% (c) $ClSO_3H$, 0°C to 120°C, Yield: 13.5% (d) 3-methyl-3-(2,4,5-trimethyl-3,6-dioxo-cyclohexa-1,4-dienyl)-butyric acid, HATU, DIEA, r.t., Yield: 6.1%.

### Preparation of 6-hydroxy-4,4,5,7,8-pentamethyl-3,4-dihydrocoumarin (1)

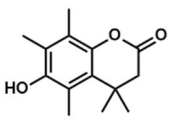


Trimethylhydroquinone (3.04 g, 20.0 mmol) and 3-methylcrotonic acid (2.20 g, 22.0 mmol) were dissolved in $MeSO_3H$ (15 mL), and the solution was stirred at 85°C for 6 h under Ar. Then, the mixture was cooled to r.t. and the product was extracted with AcOEt and washed with sat.$NaHCO_3$ aq.. The organic layer was evaporated to dryness and pumped up to afford

**1** (4.70 g, 20.1 mmol, quant yield).
$^{1}$H NMR (400 MHz, $CDCl_3$): δ 1.44 (s, 6H), 2.17 (s, 3H), 2.20 (s, 3H), 2.34 (s, 3H), 2.53 (s, 2H), 4.73 (s, 1H).
$^{13}$C NMR (100 MHz, $CDCl_3$): δ 12.4, 12.7, 14.6, 26.7, 27.8, 35.6, 46.2, 119.0, 121.9, 123.5, 128.3, 143.6, 148.9, 169.0.
HRMS ($ESI^+$): Calcd. for $[M+H]^+$ 235.13342, Found 235.13197 (-1.5 mmu).

**Preparation of 3-methyl-3-(2,4,5-trimethyl-3,6-dioxo-cyclohexa-1,4-dienyl)-butyric acid (2)**

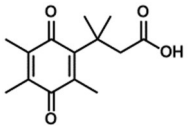

Compound **1** (4.70 g, 20.1 mmol) was dissolved in MeCN/$H_2O$ (6/12 mL), and then N-bromosuccinimide (NBS, 3.86 g, 21.7 mmol) was added. The mixture was stirred at r.t. for 2 h, then the mixture was extracted with AcOEt/2N HCl aq. and evaporated to dryness. The residue was purified by MPLC (silica, eluent, 50% $CH_2Cl_2$/hexane (0 min) to 100% $CH_2Cl_2$/hexane (9 min)) to afford **2** (3.86 g, 15.4 mmol, 76.7 % yield).
$^{1}$H NMR (400 MHz, $CDCl_3$): δ 1.33 (s, 6H), 1.82 (s, 3H), 1.85 (s, 3H), 2.04 (s, 3H), 2.91 (s, 2H), 10.94 (s, 1H).
$^{13}$C NMR (100 MHz, $CDCl_3$): δ 12.1, 12.5, 14.3, 28.8, 37.9, 47.3, 138.3, 139.0, 143.0, 152.1, 178.7, 187.4, 190.8.
HRMS ($ESI^-$): Calcd. for $[M-H]^-$ 249.11268, Found 249.10864 (-4.1 mmu).

**Preparation of 7-amino-2-oxo-4-(sulfomethyl)-2*H*-chromene-6-sulfonic acid (3, dsAMC)**

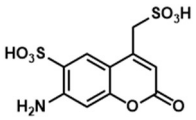

$ClSO_3H$ (2 mL) was added slowly to 7-amino-4-methylcoumarin (554 mg, 3.16 mmol) at 0°C and the mixture was stirred at 120°C for 4 h. The mixture was cooled to 0°C and quenched with $H_2O$ and neutralized with 2N NaOH aq. The residue was purified by HPLC (eluent, 4% $CH_3CN$/0.1% TEAA aq. (0 min) to 80% $CH_3CN$/0.1% TEAA aq. (25 min); flow rate = 5.0 mL/min) and desalted with $H_2O$ to afford **3** as a triethylamine salt (230 mg, 0.43 mmol, 13.5 % yield).
$^{1}$H NMR (400 MHz, $CD_3OD$): δ 4.19 (s, 2H), 6.18, (s, 1H), 6.63 (s, 1H), 8.20 (s, 1H).
$^{13}$C NMR (100 MHz, $CD_3OD$): δ 52.5, 100.9, 108.2, 111.4, 125.5, 126.4, 149.3, 149.4, 156.5,

162.0.
HRMS (ESI$^-$): Calcd. for [M-H]$^-$ 333.96913, Found 333.96614 (-3.0 mmu).

**Preparation of compound 4 (Q-dsAMC)**

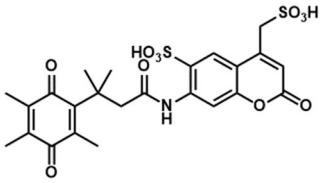


Compound **3** (54 mg, 0.10 mmol), compound **2** (73.5 mg, 0.29 mmol), HATU (108 mg, 0.28 mmol) and DIEA (81 μL, 0.47 mmol) were dissolved in MeCN (1 mL). The mixture was stirred at r.t. for 16 h, and evaporated to dryness. The residue was purified by HPLC (eluent, 4% $CH_3CN$/0.1% TEAA aq. (0 min) to 80% $CH_3CN$/0.1% TEAA aq. (25 min); flow rate = 5.0 mL/min) and desalted with $H_2O$ to afford **4** as a triethylamine salt (4.7 mg, 0.0061 mmol, 6.1 % yield).
$^1$H NMR (400 MHz, DMSO-$d_6$): δ 1.38 (s, 6H), 1.92 (s, 3H), 1.95 (s, 3H), 2.05 (s, 3H), 2.95 (s, 2H), 3.86 (s, 2H), 6.25 (s, 1H), 8.08 (s, 1H), 8.09 (s, 1H), 10.61 (s, 1H).
HRMS (ESI$^-$): Calcd. for [M+Na-2H]$^-$ 588.06102, Found 588.06169 (+0.7 mmu).

## Supplementary Tables

**Table S1.** Reports about the upregulation of glyoxalase system activities in various tumor cells.

| Cancer | Upregulation | Cell growth | Reference |
|---|---|---|---|
| Gastric cancer | GLO1 gene | Inhibition by BBGCD (*in cellulo*) | *Oncogene*, **2015**, *34*, 1196-1206. |
| Breast cancer | GLO1 mRNA and protein | Inhibition by siRNA (*in cellulo*) | *Int. J. Clin. Exp. Pathol.*, **2017**, *10*, 10852-10862. |
| Prostate cancer | GLO1 activity | Inhibition by BBGCD (*in cellulo* and *in vivo*) | *Clin. Cancer Res.*, **2001**, *7*, 2513-2518. |
| Melanoma | GLO1 mRNA | Inhibition by siRNA (*in cellulo*) | *Melanoma Res.*, **2010**, *20*, 85-96. |
| Hepatocellular carcinoma | GLO1 mRNA | Inhibition by shRNA (*in cellulo* and *in vivo*) | *Int. J. Clin. Exp. Pathol.*, **2014**, *7*, 2079-2090. |
| Lung cancer (NSCLC, SCLC) | GLO1 activity | Inhibition by BBGCD (*in cellulo* and *in vivo*) | *Clin. Cancer Res.*, **2001**, *7*, 2513-2518. |
| Leukimic stem cells ($Bcr\text{-}Abl^+$) | GLO1 activity | Inhibition by BBGCD (*in cellulo*) | *Cell Death Differ.*, **2010**, *17*, 1211-1220. |
| Breast cancer (Triple negative) | GLO1 activity | Not Determined | *Oncotarget*, **2012**, *5*, 5472-5482. |
| Pancreatic cancer | GLO1 protein | Not Determined | *Anticancer Res.*, **2012**, *32*, 3219-3222. |
| Leukemia (apoptosis-resistant UK711 and UK110 cells) | GLO1 mRNA | enhanced etoposide-induced apoptosis by cotreatment with BBGCD (*in cellulo*) | *Blood*, **2000**, *95*, *3214-3218.* |

**Table S2.** List of currently available assays to monitor glyoxalase activities[1].

| | Detection of metabolite | Method | Throughput | Assay |
|---|---|---|---|---|
| **Glyoxalase 1 activity** | *S*-D-lactoylglutathione | Spectrophotometric assay at 240 nm | High | *In vitro* |
| | | LC-MS | Low | *In vitro* |
| **Glyoxalase 2 activity** | *S*-D-lactoylglutathione | Spectrophotometric assay at 240 nm | High | *In vitro* |
| | | LC-MS | Low | *In vitro* |
| | GSH | LC-MS | Low | *In vitro* |
| | D-lactate | LC-MS | Low | *In vitro* |

**Table S3.** Names of hit compounds and the inhibitory activity of glyoxalase system of DMS114 cells.

| Compound | Name | Activity |
|---|---|---|
| **A** | 4-nitrobenzyl ((3,4-dichlorophenyl)sulfonyl)glycinate | 50% |
| **B** | 2-((4-chloro-1-(4-chlorophenyl)-2,5-dioxo-2,5-dihydro-1*H*-pyrrol-3-yl)amino)benzoic acid | 99% |
| **C** | 5-hydroxy-2-(2-isobutyl-1,3-dioxoisoindoline-5-carboxamido)benzoic acid | 60% |
| **D** | 3,4-dichloro-N-(4-oxo-4,5-dihydrothiazol-2-yl)benzamide | 77% |
| **E** | 2,2'-((3,5-di-tert-butyl-4-hydroxybenzyl)azanediyl)bis(ethan-1-ol) | 58% |
| **F** | 5-chloro-1-methyl-1H-benzo[*d*]imidazole-2-carboxylic acid | 55% |
| **G** | 7-hydroxy-2-phenyl-4*H*-chromen-4-one | 84% |
| **H** | (*E*)-2-(1,3-dimethyl-2,6-dioxo-1,2,3,6-tetrahydro-7*H*-purin-7-yl)-*N*'-(4-(dimethylamino)benzylidene)acetohydrazide | 77% |
| **I** | 1-(5-((3,4-dimethoxybenzyl)amino)-3-(pyridin-3-yl)-1*H*-1,2,4-triazol-1-yl)-2-methylpropan-1-one | 58% |
| **J** | (*E*)-4-(5-((2-(3,5-dimethoxybenzoyl)hydrazineylidene)methyl)furan-2-yl)benzoic acid | 78% |
| **K** | 2-(indolin-1-yl)-2-oxoethyl 4-oxo-3-propyl-3,4-dihydrophthalazine-1-carboxylate | 70% |
| **L** | 2-((2-((4,5-diphenylthiazol-2-yl)amino)-2-oxoethyl)thio)acetic acid | 66% |
| **M** | 1-benzyl-3-hydroxy-2*H*-chromeno[3,4-*b*]pyrazine-2,5(1*H*)-dione | 72% |
| **N** | 7-hydroxy-6-methoxy-3-((2-oxo-2*H*-chromen-7-yl)oxy)-2*H*-chromen-2-one | 84% |
| **O** | 1-(4-chlorophenyl)-3-(pyridin-2-ylthio)propan-1-one | 58% |
| **P** | ethyl 5-(thiophen-2-yl)isoxazole-3-carboxylate | 47% |
| **Q** | 2-((2,6-dichlorobenzyl)thio)pyrazolo[1,5-*a*][1,3,5]triazin-4(3*H*)-one | 67% |
| **R** | 2-(furan-2-yl)-6-(2-isopropoxyethoxy)-4*H*-chromen-4-one | 67% |
| **S** | 2-((4-(4-methoxy-3-nitrophenyl)-5-methylthiazol-2-yl)carbamoyl)benzoic acid | 76% |
| **T** | (*S*)-*N*-(4-(1-(4,5,6,7-tetrafluoro-1,3-dioxoisoindolin-2-yl)ethyl)phenyl)acetamide | 91% |
| **U** | 3,4,5-trimethoxy-*N*-((2-oxo-1,2-dihydrobenzo[*cd*]indol-6-yl)methyl)benzamide | 72% |

**Table S4.** Parameters determined from the calibration curves of **Figure 4c** and **4d**.

**Figure 4c left (Extracellular D-lactate, NHBE cells)**

| y=m1+(m2-m1)/(1+(x/m3)^m4); | | |
|---|---|---|
| Parameters | Value | Errors |
| m1 | 56.628 | 18.835 |
| m2 | 105.13 | 2.7788 |
| m3 | 26.343 | 9.8328 |
| m4 | 2.7442 | 2.2563 |
| Chi-squared | 88.365 | NA |
| R | 0.97594 | NA |

**Figure 4c left (Extracellular D-lactate, DMS273 cells)**

| y=m1+(m2-m1)/(1+(x/m3)^m4); | | |
|---|---|---|
| Parameters | Value | Errors |
| m1 | 19.817 | 2.1699 |
| m2 | 77.934 | 1.4693 |
| m3 | 4.6432 | 0.49594 |
| m4 | 1.5385 | 0.22527 |
| Chi-squared | 11.038 | NA |
| R | 0.99859 | NA |

**Figure 4c right (Cell viability, NHBE cells)**

| y=m1+(m2-m1)/(1+(x/m3)^m4); | | |
|---|---|---|
| Parameters | Value | Errors |
| m1 | 15.034 | 4.3465 |
| m2 | 81.724 | 2.115 |
| m3 | 8.7348 | 102.35 |
| m4 | 8.8654 | 769.14 |
| Chi-squared | 53.677 | NA |
| R | 0.99477 | NA |

**Figure 4c right (Cell viability, DMS273 cells)**

| y=m1+(m2-m1)/(1+(x/m3)^m4); | | |
|---|---|---|
| Parameters | Value | Errors |
| m1 | 11.821 | 1.3531 |
| m2 | 98.114 | 1.1047 |
| m3 | 1.8677 | 0.2503 |
| m4 | 6.8326 | 1.8278 |
| Chi-squared | 10.979 | NA |
| R | 0.99956 | NA |

**Figure 4d (Cell viability, NHBE cells)**

| y=m1+(m2-m1)/(1+(x/m3)^m4); | | |
|---|---|---|
| Parameters | Value | Errors |
| m1 | 13.638 | 0.16197 |
| m2 | 90.804 | 0.27746 |
| m3 | 2.198 | 0.11052 |
| m4 | 5.4832 | 0.34062 |
| Chi-squared | 0.15397 | NA |
| R | 0.99999 | NA |

**Figure 4d (Cell viability, DMS273 cells)**

| y=m1+(m2-m1)/(1+(x/m3)^m4); | | |
|---|---|---|
| Parameters | Value | Errors |
| m1 | 5.7547 | 6.2396 |
| m2 | 101.02 | 3.8228 |
| m3 | 10.873 | 1.1907 |
| m4 | 2.8271 | 0.85925 |
| Chi-squared | 60.217 | NA |
| R | 0.99676 | NA |

## Supplementary Figures

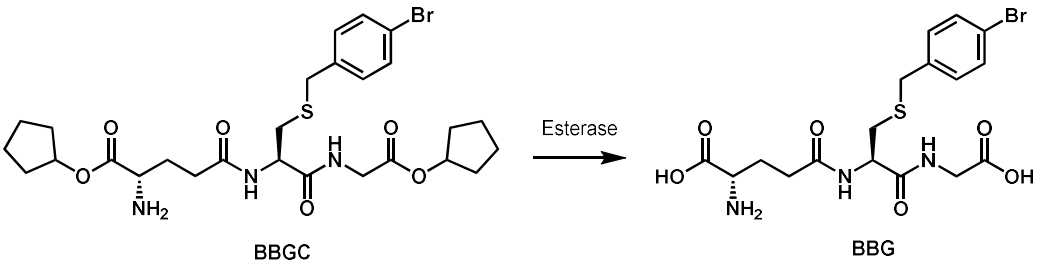


**Figure S1.** Activation of BBGC to BBG.

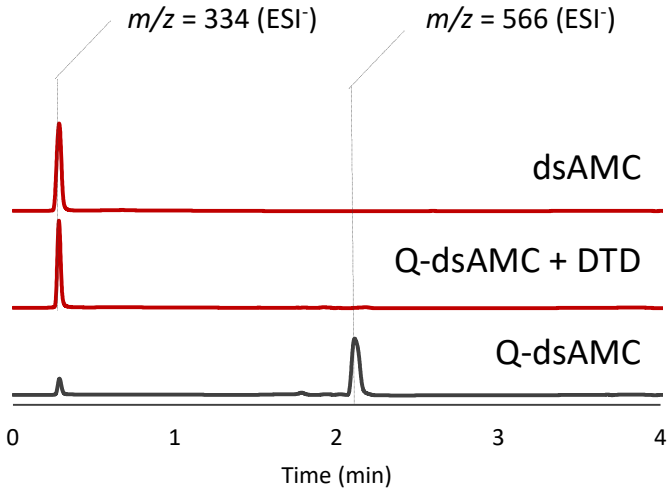


**Figure S2.** Reaction of Q-dsAMC with DT-diaphorase. LC chromatograms (λ = 320 nm) of Q-dsAMC (10 μM) after reacting with or without NADH (30 μM) and DT-diasphorase (1 U/mL) for 1 h. dsAMC is a reference product (10 μM).

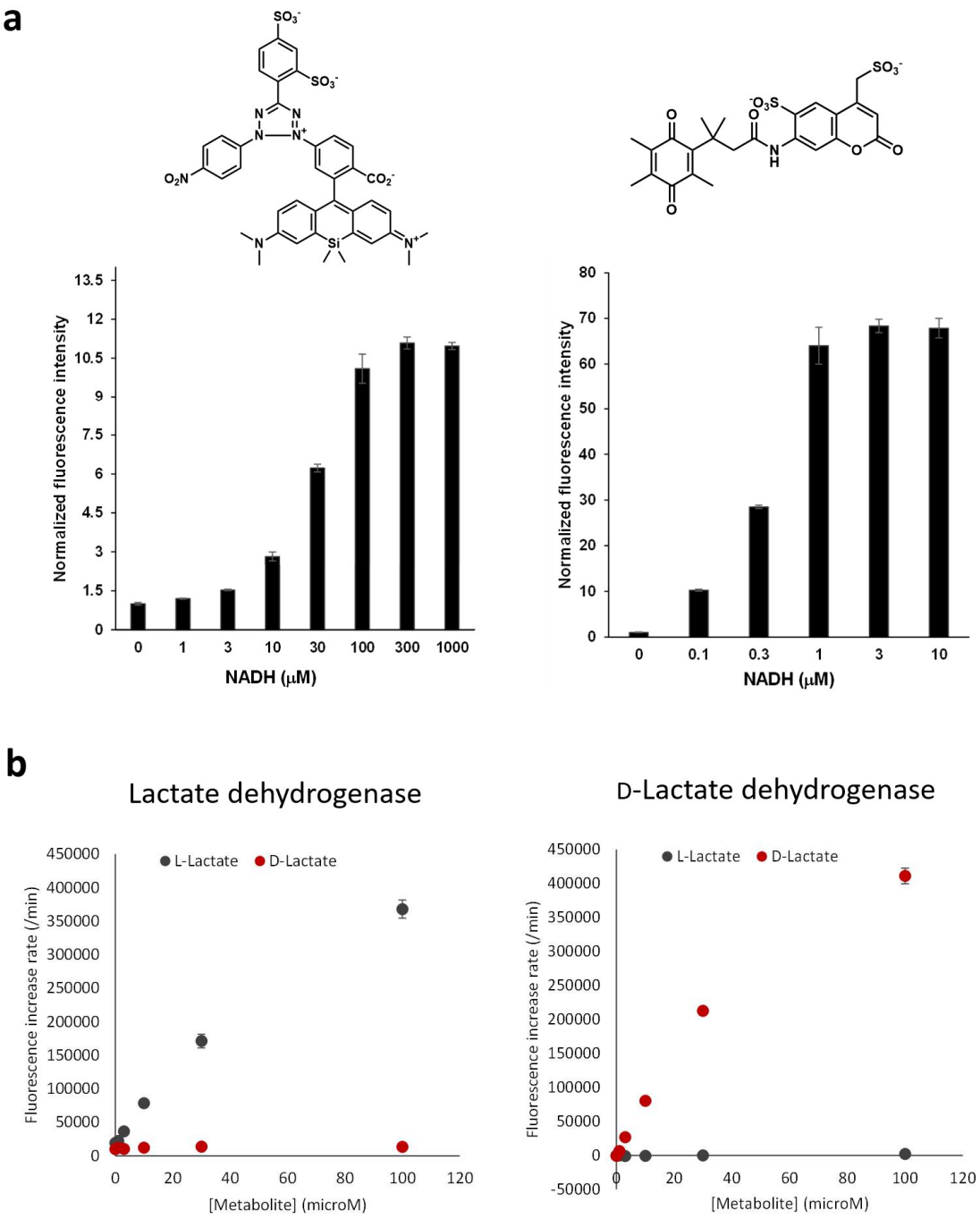


**Figure S3.** Characterization of Q-dsAMC in comparison with conventional probes used in live cell-based coupled assays. (a) Normalized fluorescence intensities of (left) SiRWST-3 (1 μM) after mixing with NADH (0-1000 μM) and 1-methoxy-PMS (10 μM) in DPBS (pH 7.4) or (right) Q-dsAMC (1 μM) after mixing with NADH (0-30 μM), DT-diaphorase (1 U/mL) in DPBS (pH 7.4). Error bars represent S.D. (n = 3). (b) Fluorescence intensities of Q-dsAMC (10 μM) after mixing with $NAD^+$ (0-100 μM), L-lactate or D-lactate (0-100 μM) with lactate dehydrogenase (left) or D-lactate dehydrogenase (right) (5 μg/mL) in PBS (pH 7.4) containing 0.1% CHAPS and incubated for 10 min. Error bars represent S. D. (n = 4).

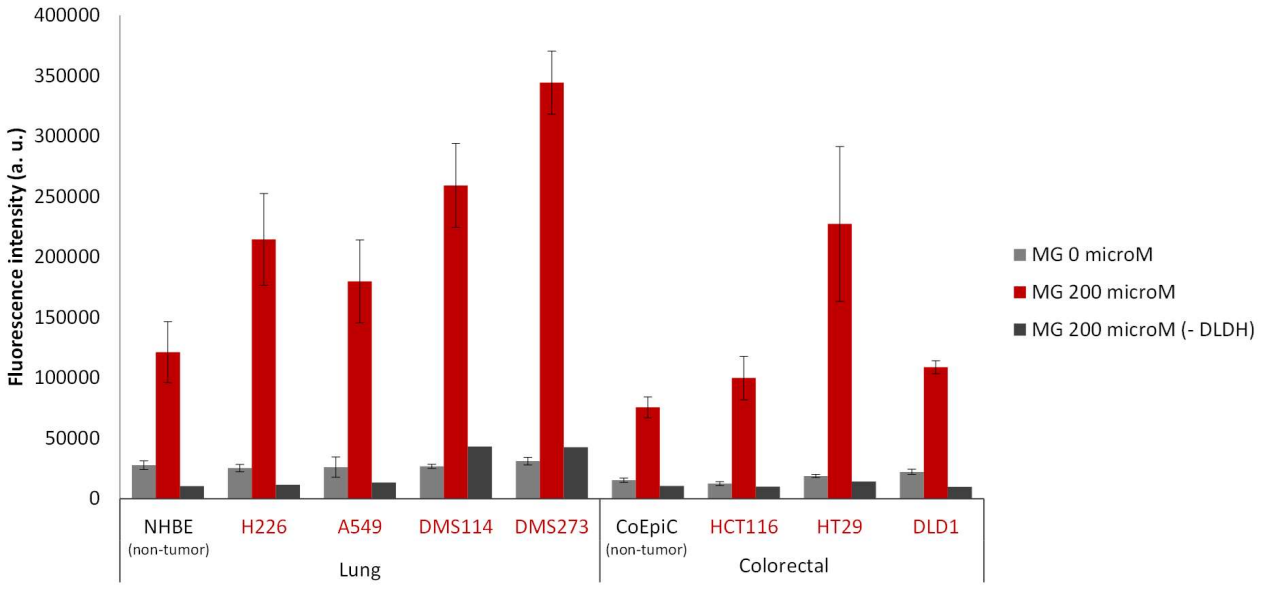


**Figure S4.** Detection of glyoxalase pathway activities in various tumor and non-tumor cells from lung and colon. Cells are incubated in DPBS (pH 7.4) containing 0 or 200 μM 2-MG with or without D-lactate dehydrogenase (DLDH, 1 U/mL). Cells ($2\times10^3$ cells) were incubated with MG (0 or 200 μM) in DPBS for 1 h at 37°C. After incubation, probe solution was added and the fluorescence intensity was measured by plate reader. Error bars represent S.D. (n = 4).

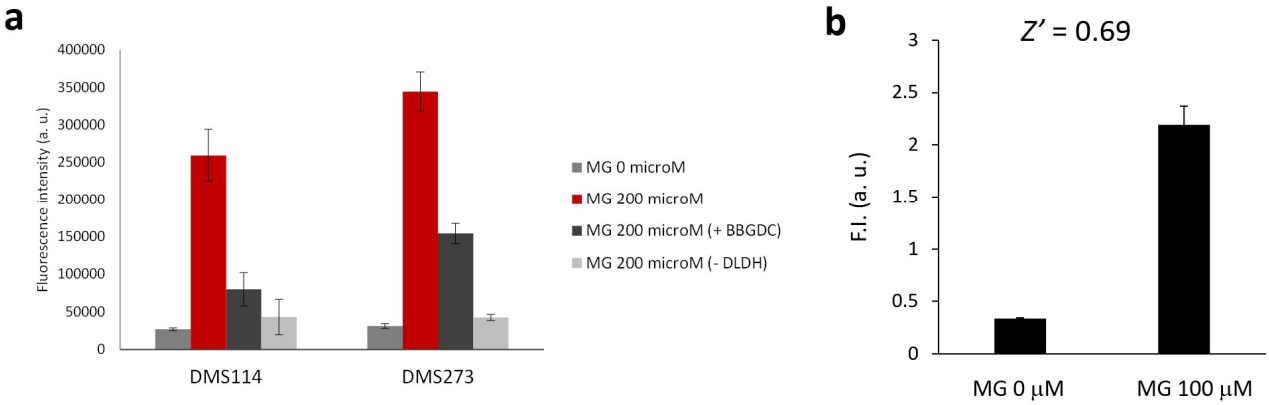


**Figure S5.** Validation of screening conditions. (a) Cells are incubated in DPBS (pH 7.4) containing 0 or 200 μM 2-MG with or without D-lactate dehydrogenase (DLDH, 1 U/mL) and with or without BBGC (50 μM). Error bars represent S.D. (n = 4). (b) Calculation of *Z'*-value. DMS114 cells ($2\times10^3$ cells) were incubated with MG (0 or 100 μM) in DPBS for 2 h at r.t.. After incubation, the equal amount of probe solution was added and the fluorescence intensity was measured by plate reader (Ex./Em.= 355/460 nm). Probe solution: Q-dsAMC (2 μM), $NAD^+$ (200 μM), DT-diaphorase (2 U/mL), DLDH (2 U/mL) in DPBS. Error bars represent S.D. n = 16 (treatment with MG 0 μM), n = 336 (treatment with MG 100 μM).

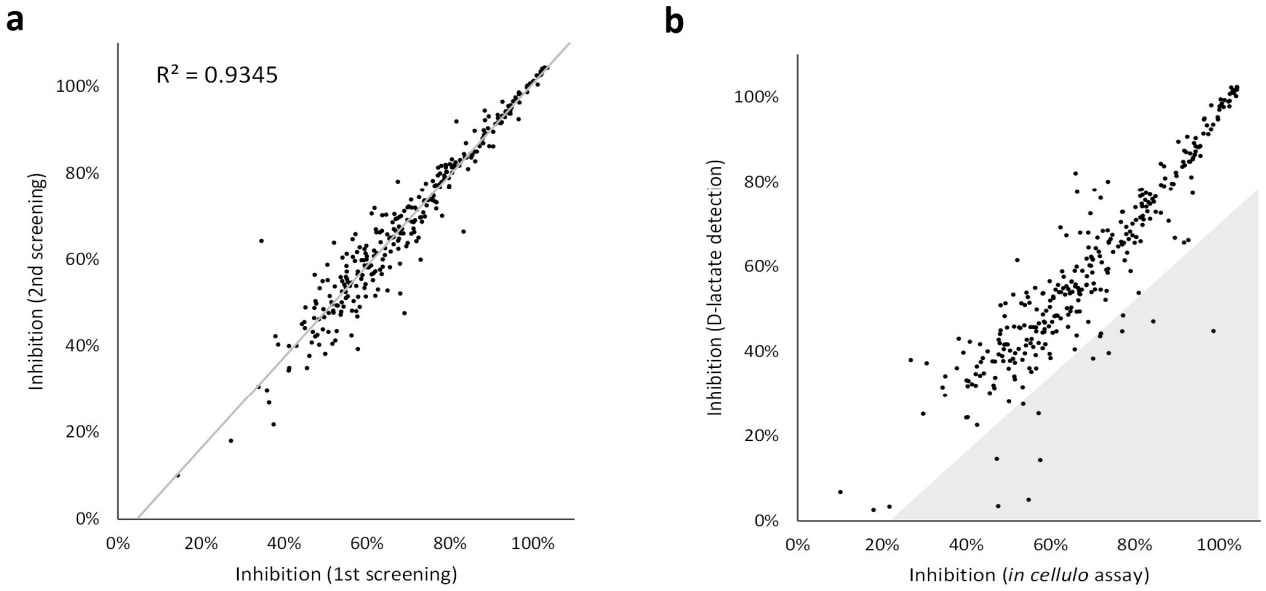


**Figure S6.** Repeatability of assay. (a) The results of 583 compounds selected as hit in 1st screening are shown. The horizontal axis indicates the inhibitory activity observed in 1st screening and the vertical axis indicates the inhibitory activity observed in 2nd screening. (b) Summary results of 2nd screening. The horizontal line indicated the inhibition in the live cell-based assay, and the vertical line indicated the inhibitory activity against D-lactate detection system. The compouds that are in gray triangle was chosen as hit comounds.

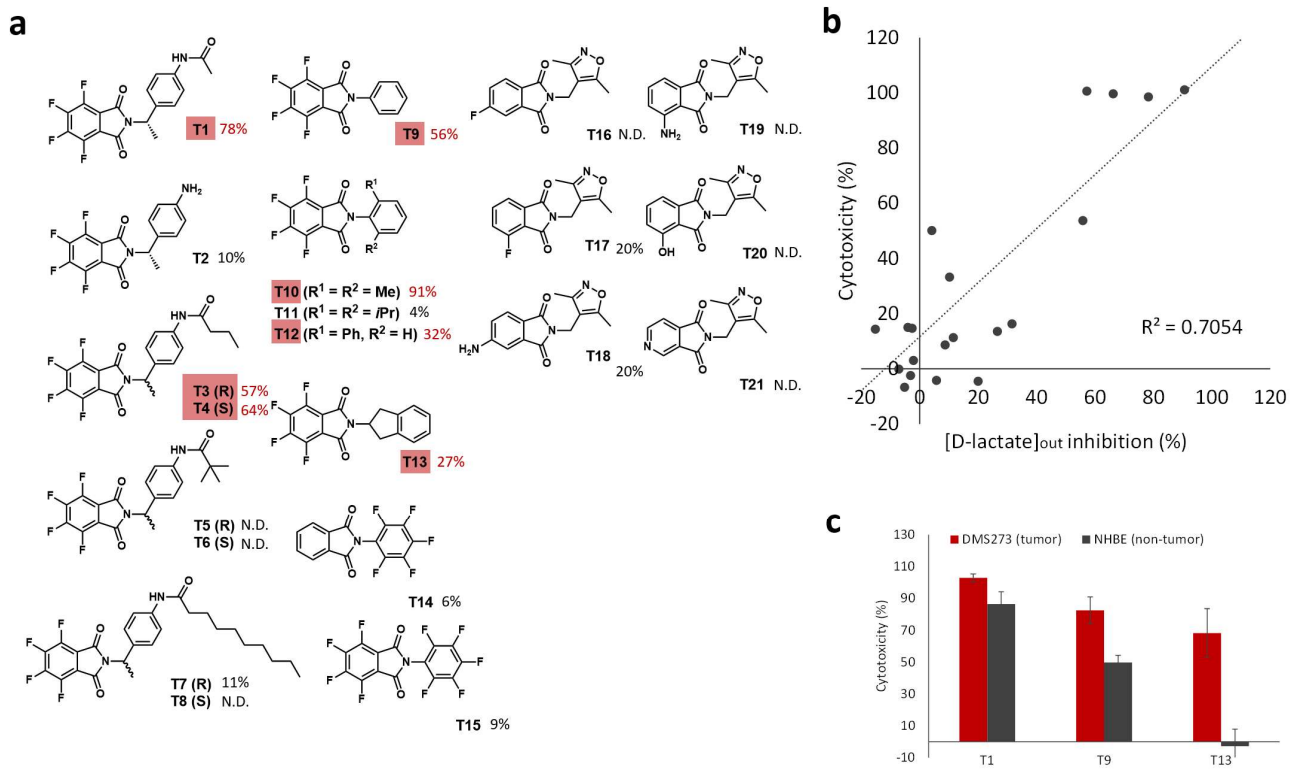


**Figure S7.** Glyoxalase pathway inhibitory activities and cytotoxicity of analogues of compound **T**. (a) Structures of analogues of compound **T** (**T1**-**T21**) and their glyoxal metabolic pathway modulatory activities (changes of extracellular D-lactate concentration) as shown in **Figure 4b**. Correlation of metabolic modulating activities (horizontal) and cytotoxicity (viability after 48 h, vertical) of **T1**-**T21** for DMS114 cells. (c) Cytotoxicity of compound **T1**, **T9** and **T13** toward DMS273 cells and NHBE cells. Error bars represent S.D. (n = 3).

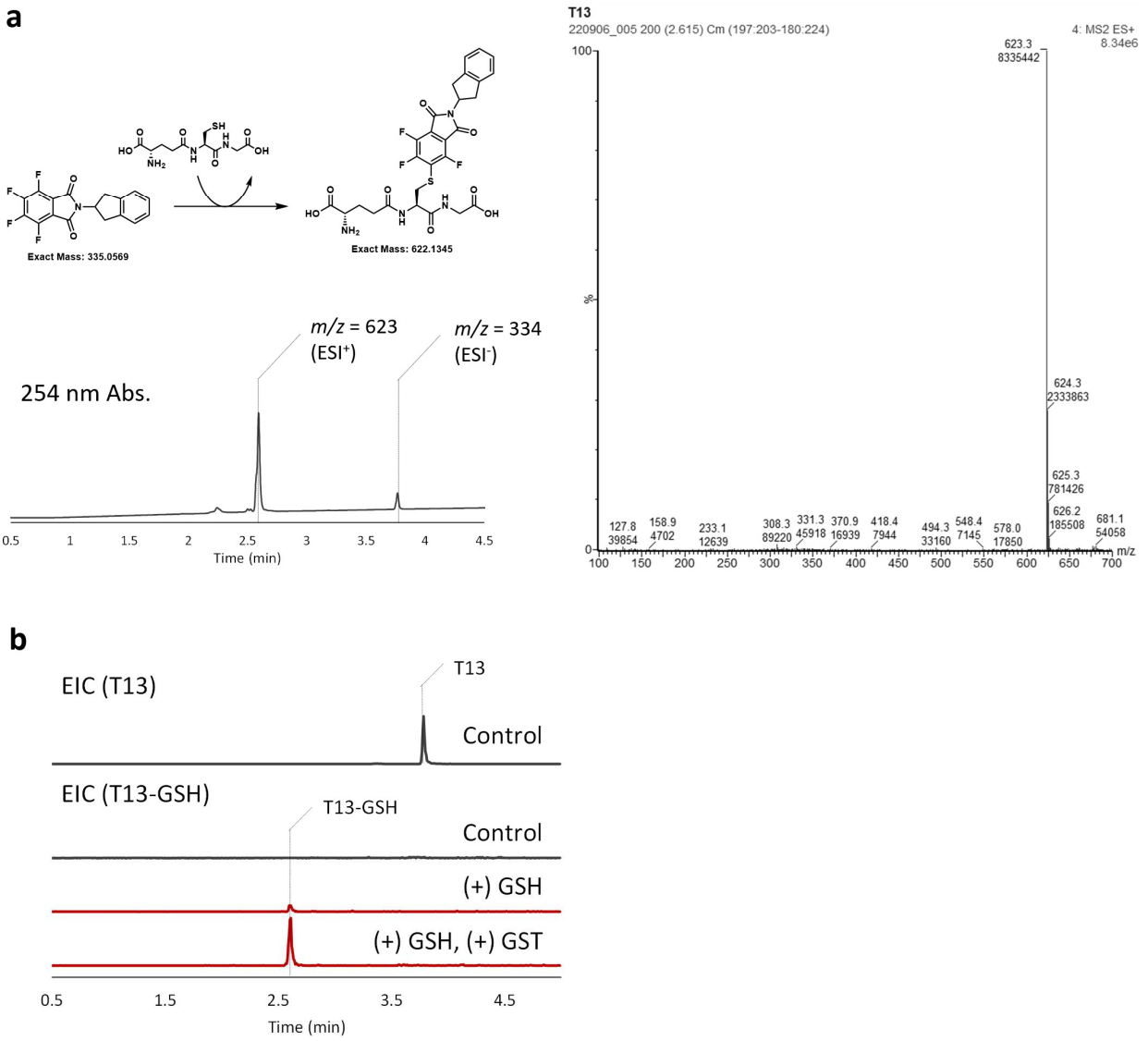


**Figure S8.** Tetrafluorophthalimides as GST-dependent GSH reacting reagents. (a) (left) LC-MS chromatogram of **T13** (100 μM) reacting with GSH (1 mM) in DMSO for 1 h. (right) Mass spectrum (ESI+) observed at 2.6 min. (b) Multiple reaction monitoring (MRM) chromatograms of **T13** (10 μM) reacting with or without GSH (1 mM) and glutathione *S*-transferase Pi (10 μg/mL) at 37˚C for 1 h. MRM conditions were constructed for **T13** (*m/z* = 336.1 > 117.1 (ESI+)) and **T13** reacted with glutathione in DMSO (*m/z* = 623.3 > 117.3, 391.1 (ESI+)).

## Supplementary References

1 N. Rabbani, M. Xue and P. J. Thornalley, *Clin. Sci.*, 2016, **130**, 1677–1696.